 doi:10.20944/preprints202112.0128.v1

Article

IN-VITRO AND IN-VIVO FEASIBILITY STUDY FOR A MOBILE VV-ECMO AND ECCO$_2$R SYSTEM

Lasse J. Strudthoff[1,*], Hannah Lüken[2], Sebastian V. Jansen[1], Jan Petran[2], Peter Schlanstein[1], Lotte Schraven[1], Benjamin J. Schürmann[1], Niklas B. Steuer[1], Georg Wagner[1], Thomas Schmitz-Rode[4], Ulrich Steinseifer[1], Jutta Arens[1,3,¶] & Rüdger Kopp[2,¶]

[1] Department of Cardiovascular Engineering, Institute of Applied Medical Engineering, Medical Faculty, RWTH Aachen University, Aachen, Germany
[2] Clinic for Intensive Care Medicine, Medical Faculty, University Hospital RWTH Aachen, Aachen, Germany
[3] Chair in Engineering Organ Support Technologies, Department of Biomechanical Engineering, Faculty of Engineering Technologies, University of Twente, Enschede, The Netherlands
[4] Institute of Applied Medical Engineering, Medical Faculty, RWTH Aachen University, Aachen, Germany
[¶] Equal contribution
[*] Correspondence: strudthoff@ame.rwth-aachen.de

Abstract: Extracorporeal membrane oxygenation (ECMO) is an established rescue therapy for patients with chronic respiratory failure waiting for lung transplantation (LTx). The therapy inherent immobilization may result in fatigue, consecutive deteriorated prognosis and even lost eligibility for transplantation. We conducted a feasibility study on a novel system designed for the deployment of a mobile ECMO device, enabling physical exercise of awake patients prior to LTx. The system comprises a novel mobile oxygenator with a directly connected blood pump, a double lumen cannula, gas blender and supply, as well as control, and energy management. In-vitro experiments included tests regarding performance, efficiency, and blood damage. A reduced system was tested in vivo for feasibility using a novel large animal model. Six anesthetized pigs were first positioned in supine position, followed by a 45° angle, simulating an upright position of the patients. We monitored performance and vital parameters. All in-vitro experiments showed good performance for the respective subsystems and the integrated system. The acute in-vivo trials of 8h duration confirmed the results. The novel mobile ECMO-system enables adequate oxygenation and decarboxylation sufficient for, e.g., physical exercise of designated LTx-recipients. These results are promising and suggest further preclinical studies on safety and efficacy to facilitate translation into clinical application.

Keywords: ECMO; ECLS; ECCO$_2$R; ARDS; respiratory failure, LTx, DIN EN ISO 7199; Extracorporeal membrane oxygenation, acute respiratory distress syndrome, animal model

1. Introduction

Veno-venous extracorporeal membrane oxygenation (VV-ECMO) is an established therapy for patients with severe acute respiratory distress syndrome [1]. For patients with irreversible respiratory failure, a lung transplantation (LTx) is the last resort measure [2]. For gas exchange in decompensated patients before LTx, ECMO as well as low flow extracorporeal CO_2 removal (ECCO$_2$R) has become an established strategy as so-called bridge to (lung) transplantation [3–6]. Worldwide, 328 Mio. Patients [7] suffer from advanced chronic obstructive pulmonary disease (COPD). A growing number, currently 10 Mio. patients [8], suffers from advanced GOLD III/IV COPD status, resulting in 30.1 % of all LTx [9,10]. Due to organ shortage, the waiting time for a suitable organ is 446±517 days [11], during which time at least 10 % of the patients lose therapy eligibility or decease [12,13]. Conventional treatment prior to LTx includes drug treatment and mechanical ventilation. The efficacy of this treatment is limited mostly due to ventilator induced lung injury (VILI) as well as sedation and immobilization of the patients in the

Preprints (www.preprints.org) | NOT PEER-REVIEWED | Posted: 8 December 2021 doi:10.20944/preprints202112.0128.v1

intensive care unit. Immobilized patients go through a sequence of physical deteriorations comprising muscle atrophy, (poly-)neuroatrophy, and finally a state of general fatigue and deterioration of the general condition [14–16]. This deterioration means either losing the eligibility for, or dramatically worsen the outcome of the intended LTx [17]. VV-ECMO was established as an alternative or adjuvant therapy to decrease the detrimental effects of mechanical ventilation [18]. However, the immobilization of the patients remains a problem, as current ECMO-systems are complex, heavy, bulky, require highly trained medical staff, and are prone to technical complications like cannula kinking. First approaches to mobilize patients have been undertaken [12,19–23]. The results of these studies have been promising, yet, the resource intensity for the mobilization of patients is immense: Haji et al. recently published their physical exercise protocol, involving seven medical staff members for out-of-bed mobilization [24].

Within the present paper, we report results of a feasibility study for a mobile VV-ECMO system. The system comprises a double lumen cannula, an integrated pump-oxygenator-unit, mobile gas supply utilizing ambient air, a battery system and a carrying modality. The concept is depicted in **Figure 1**. All components were individually tested and characterized by respective in-vitro tests. The entire system was tested in vivo in porcine animal trials. We demonstrated an effective system in terms of mobility, therapy-relevant parameters including gas and heat transfer, and interoperability of all components.

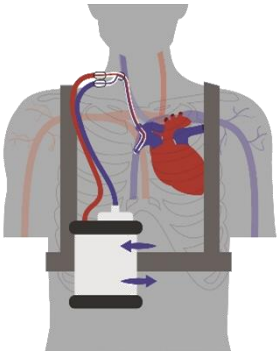

***Figure 1** - Concept for a mobile VV-ECMO system*

2. Materials and Methods

The mobile VV-ECMO system comprises specifically designed prototypes of the oxygenator, energy supply, control unit, gas blender and pump drive, driving a commercially available blood pump. All predefined parameters for a double lumen cannula were met by a commercially available product. All components are described below. These components were tested individually in-vitro following relevant norms and guidelines (ISO 7199 [25]; Guidance for Cardiopulmonary Bypass Oxygenators 510(k) Submissions; Final Guidance for Industry and FDA Staff [26]). The integrated system was tested in a novel large animal test model. **Figure 2** shows a prototype system and the intended carrying mode.

Preprints (www.preprints.org) | NOT PEER-REVIEWED | Posted: 8 December 2021 doi:10.20944/preprints202112.0128.v1

Figure 2 *- Prototype system of mobile VV-ECMO system*

2.1. System components

For the double lumen cannula, we chose the Novaport Twin (Xenios AG, Germany, now Fresenius SE & Co. KGaA). The cannula is designed for the right external jugular access with in- and outlet situated in the superior vena cava and in front of the right atrium, respectively. The positioning of drainage and reperfusion openings of the cannula was developed to mitigate blood recirculation. With an outer diameter of 22 Fr and 3/8" connectors, the cannula was designed to allow a blood flow of up to 3 l/min with a pressure drop below 140 mmHg, based on standard requirements for VV-ECMO of the described group of patients. The cannula has a minimum kink resistance to guarantee safety during patient mobilization (< 50 % flow reduction during 180° kinking with kinking radius of 35 mm). Since we used a commercially available cannula, we did not evaluate the hemolysis in vitro.

As energy supply for the control system, the gas blender and the pump drive, commercially available 11.25 V, 2.95 Ah rechargeable battery packs with three lithium-ion cells were installed (RRC2040, RRC Power Solutions GmbH, Germany). These battery packs are characterized by quick charging, extended life span, impedance tracking, cell balancing and do not require manual recalibration. Due to a high energy density, they have a low weight of 170 g and small dimensions of 85 mm x 59 mm x 22 mm per unit, do not produce extensive heat and can be used in acceptable temperature ranges for patient ambulation.

As pump, a conventional DP3 with an altered pump drive was utilized (Xenios AG, Germany, now Fresenius SE & Co. KGaA). The drive was miniaturized in size and weight (425 g) and, during prototype development stage, situated at the casing of the oxygenator unit. This allowed for a direct connection to the specially designed inlet of the oxygenator unit without any tubing. The DP3 pump produces a pressure head of 600 mmHg at flows far above the intended 3 l/min at max. 10,000 rpm.

The oxygenator unit was designed to achieve a flow of 3 l/min with an acceptable maximum pressure drop of around 100 mmHg (**Figure 3**). Further, the gas transfer efficacy should reach 150 ml/min for O_2 and CO_2, requiring a membrane surface of around 0.75 m^2, based on data interpolations of existing stacked oxygenators. The fibers were arranged in stacks with solid polymethylpentene-membranes for gas transfer and polyethylenterephthalat-membranes for heat exchange (OxyPlus 90/200 single knitted loop mat and Hexpet 60/670 single distorted knitted loop mat, both Membrana GmbH, Germany). Heat transfer may be necessary despite the miniaturized circuit due to extracorporeal circulation. The extent of this has not been object of the current study. During mobilization sequences, the heat exchange fibers were not active. The phase separation was implemented using a state-of-the-art centrifugal potting process [27] with

Preprints (www.preprints.org) | NOT PEER-REVIEWED | Posted: 8 December 2021 doi:10.20944/preprints202112.0128.v1

silicone (Elastosil 620, Wacker Chemie AG, Germany) and a resulting flow path diameter of 8.5 cm. The oxygenator unit also incorporates a gas bubble trap. For this early prototype, a 3D-printed casing was used. The oxygenator has a total weight of around 650 g. Targeted blood cell damage and heat transfer are within the range of commercially available VV-ECMO-systems. Corresponding experiments are described below.

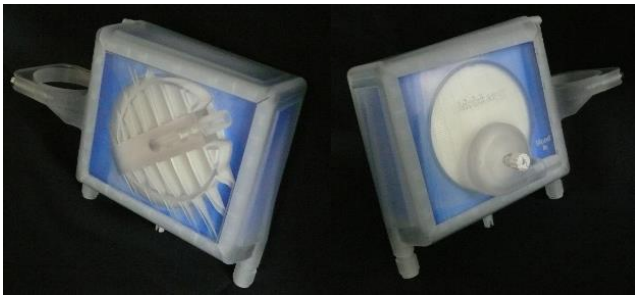

Figure 3 *- Novel mobile, stacked, centrifugal potted membrane oxygenator front and back*

The gas blender comprises pneumatic components to blend ambient air with pressurized medical oxygen including a pneumatic pump, (unidirectional) valves, air filters, pressure regulators, and a flow control system (**Figure 4**). The system can produce 10 l/min of flow with a FiO_2 between 0 and 100 % at a pressure head of 60 mmHg. The gas blender unit also contains the overall control system.

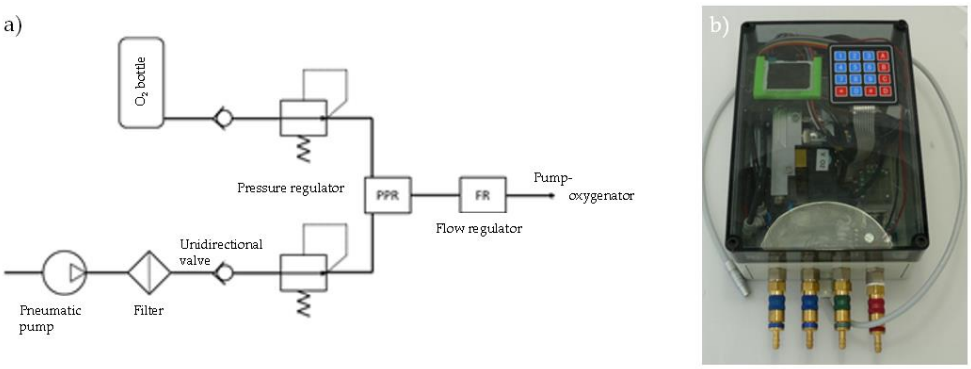

Figure 4 *a) gas blender schematic, b) gas blender prototype*

2.2. In-vitro evaluation

Oxygenator pressure drops, oxygen and carbon dioxide transfer rates, heat exchanger performance factor (R-value), and blood cell damage were evaluated in-vitro according to ISO 7199 [25] and FDA guideline [26]. Eleven full scale gas transfer tests were conducted with each six identical circuits including prototypes of the novel oxygenator and pooled, anticoagulated, porcine blood. The feed gas composition and blood/gas-flow ratio was different in each of the six circuits (all possible combinations with FiO_2 = 21 %, FiO_2 = 50 %, FiO_2 = 100 % and 4 : 1 gas/blood, 1 : 1 gas/blood). For hemolysis testing, an iLA membrane oxygenator in combination with a conventional DP3 pump (Xenios AG, Germany, now Fresenius SE & Co. KGaA, Germany) was used as predicate device in comparison to five identical prototypes of the novel oxygenator.

2.3. In-vivo evaluation

To verify the function of our newly designed prototype for mobile ECMO, six acute animal trials were conducted using 50 - 80 kg female pigs of the German Landrace. Permission for the experiments was granted by the governmental animal care committee (Landesamt für Natur, Umwelt und Verbraucherschutz Nordrhein-Westfalen,

Preprints (www.preprints.org) | NOT PEER-REVIEWED | Posted: 8 December 2021 doi:10.20944/preprints202112.0128.v1

Recklinghausen, Germany, ref. no. 84-02.04.2016.A472), and the implementation followed the principles of laboratory animal care.

After arrival, the animals were examined by a veterinarian and held at least seven days in the stables of the institute of laboratory animal science of the Uniklinik RWTH Aachen for acclimatization. 12 hours before experiment, they were kept fasting with free access to water.

The sober pigs were premedicated with atropine (1 ml 1 %), azaperone (0.2 ml/kg) and ketamine (0.1 ml/kg) and anesthetized with propofol (initial bolus 1 mg/kg and 5 - 10 mg/kg/h) and fentanyl (8 - 12 µg/kg/h). The pigs were further treated following standard protocols of intensive care. This included the treatment of electrolyte imbalances, administration of crystalloid and colloid solutions as well as medications to sustain hemodynamic stability. Throughout the trial, an ACT of ≥ 150 sec was targeted using intravenous heparin. With the onset of general anesthesia, mechanical ventilation was initiated (tidal volume = 10 ml/kg, positive end expiratory pressure = 5 mbar, inspiratory-to-expiratory ratio = 1 : 2, and a respiratory frequency = 14 ± 4/min, following the target parameter P_aCO_2 of 35 - 45 mmHg). An arterial line was placed via one femoral artery and a pulmonary arterial catheter was placed via one jugular vein to measure cardiac output, central venous pressure, and pulmonary artery pressure continuously as well as pulmonary capillary wedge pressure discontinuously (Edwards Lifesciences, Irvine, California) using a AS/3 Compact monitor (Datex-Ohmeda, Helsinki, Finland) and a Vigilance monitor (Edwards Lifesciences). A bladder catheter was maintained to collect urine for the control of the renal function. The animals received infusions of 1 ml/kg/h Sterofundin (B.Braun, Melsungen, Germany) for fluid replacement. Afterwards, either the contralateral femoral vein or the right external jugular vein was cannulated with the NovaPort dual lumen cannula. After one bolus of 5,000 IU Heparin, the prefilled ECMO was connected and blood flow was started.

The experimental sequence plan is depicted in **Figure 5** and described in the following paragraph.

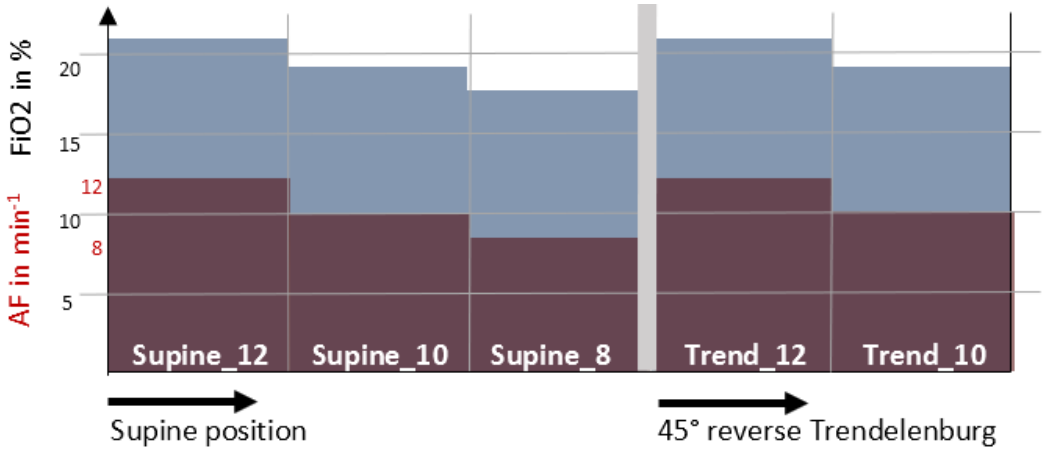

***Figure 5** - Experimental sequence plan. Fully anesthetized pigs were supported by intermittent mechanical ventilation with an initial respiratory rate >12 min^{-1} and F_iO2 of > 21%. The sequence plan shows incremental decreases of these values to model hypercapnic and hypoxic respiratory failure. After holding each plateau for 30 minutes, blood samples were taken. ECMO-support was adjusted to stabilize the vital parameters for each plateau. During the first three measurement points, the animal was lying in supine position, followed by a simple simulation of a mobilized patient by changing to 45° reverse Trendelenburg position (see **Figure 6**)*

The experimental protocol provided an 8 h timeline from ECMO connection with fixed time points of measurements, blood samplings, and mode changing from lying to upright position and back. The animal model contains an induced hypercapnic and

Preprints (www.preprints.org) | NOT PEER-REVIEWED | Posted: 8 December 2021 doi:10.20944/preprints202112.0128.v1

hypoxic respiratory failure by lowering the F_iO_2 and the respiration frequency using the P_aO_2 and P_aCO_2 as target parameters, originally published by Kopp et al. 2016 [28]. First, animals were ventilated with an F_iO_2 of 0.21 and a respiratory rate of 12 min^{-1}. By reducing the F_iO_2 to 20 % and 18 % and correspondingly the respiratory rate to 10 and 8 min^{-1}, we generated a standardized hypoxemia and hypercapnia to simulate respiratory failure. The ECMO was running as low as possible and was adjusted according to the respective measured values with a target arterial oxygen saturation of ≥ 90 % and a target arterial carbon dioxide partial pressure of 40 - 50 mmHg. Blood gas analysis and hemodynamic parameters were measured every 30 min, before further reduction of F_iO_2 and respiratory rate. During this process, the ECMO was initially tested running with ambient air; then the feed gas was blended with oxygen to meet the physiologic oxygen demand.

The test protocol contained two distinctions: First, the pigs were brought up from supine position to a 45° reverse Trendelenburg position, simulating an upright patient as well as possible, taking into account the limitations of acute large animal models (represented on right side of **Figure 5**, depicted in **Figure 6**). In this model, dilated veins during general anesthesia in combination with gravity may cause a distributive shock. This problem was counteracted by decreasing the passive volume of the abdominal venous reservoir by abdominal compression. The second distinction regards the blending of medical oxygen with ambient air. The feed gas was altered during the course of the experiments, to see the impact of lower F_iO_2. Upon experiment finalization, animals were euthanized.

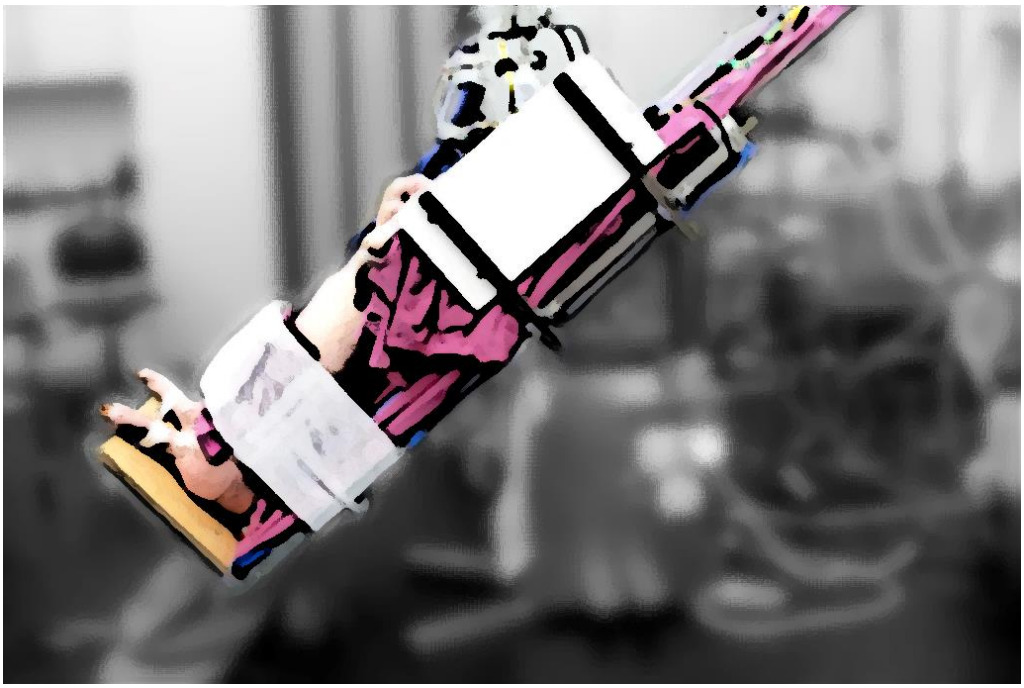

***Figure 6** - 45° Reverse Trendelenburg position with abdominal compression. The animals were placed on the operating table, a robust board was mounted below their back hooves, the compression strap was tightened around the animal abdomen and the operating table*

During the in-vivo experiments, the system and its components were tested on overall handling and performance, including vital parameters of the pigs. Oxygenator and pump unit were tested regarding gas transfer, pressure heads and drops, and hemolysis. Gas transfer was tested taking blood samples pre and post oxygenator. Hemolysis was tested every half-hour to calculate the normalized index of hemolysis (NIH) without a predicate reference device.

2.4. Statistical analysis

Preprints (www.preprints.org) | NOT PEER-REVIEWED | Posted: 8 December 2021 doi:10.20944/preprints202112.0128.v1

For in-vitro experiments, all results are depicted with mean and standard deviation (SD). Hemolysis values from the in-vitro experiments were tested for significance comparing the five test objects against the single control circuit. First, normal Gaussian distributions were tested using the Kolmogorov and Smirnov method. P-values above 0.10 were considered normal Gaussian distributions. Then, we conducted a two-tailed one sample t-test; a p-value < 0.05 was considered significant.

The in-vivo experiments were evaluated by calculating median, mean, and standard deviation. If more than one sample point was recorded within a group, their mean was calculated before the actual evaluation. All parameters shown in the result section (**Table 1**) were tested for significant differences between the five groups of the experimental sequence plan (**Figure 5**) using the Friedmann test with post Dunn's test. Two animals had no data in a single group; these values were imputed using the mean of the remaining group. If more than one value was missing for a single parameter, an unpaired Kruskal Wallis test was conducted instead. Here, a post test was not required due to insignificant results. For all tests, a p-value < 0.05 was considered significant.

3. Results

The resulting system is depicted in **Figure 2**. All predefined criteria for the mobile utilization of ECMO-patients were met. The system showed efficacy during in-vitro experiments and in-vivo trials.

3.1. In-vitro evaluation

The internal resistance of the extracorporeal circuit to blood flow is mainly caused by the cannula (properties available from manufacturer) and the oxygenator. The stacked fiber mat design results in a pressure drop of around 75 mmHg (± 20) at a blood flow rate of 3 l/min, see **Figure 7**. The integrated heat exchanger fibers allow for a heat transfer of R = 0.24 (±0.04) at the same blood flow, see **Figure 8**. The in-vitro blood tests yielded a threefold normalized index of hemolysis (NIH) of the novel device compared to a reference device (**Figure 9**).

Carbon dioxide and oxygen transfer rates are depicted in **Figure 10** and **Figure 11**, respectively. CO_2 transfer rates at 3 l/min were 110 ml/min with a flow ratio for gas/blood flows = 1 : 1. The transfer rates increase to 160 ml/min with a ratio for gas/blood flow = 4 : 1. The rates were almost independent of the oxygen fraction. The oxygen was transferred with 50 ml/min, 110 ml/min, and 160 ml/min for oxygen fractions of 21 %, 50 %, and 100 %, respectively. The oxygen transfer was almost independent of the ratio for gas/blood flows.

Preprints (www.preprints.org) | NOT PEER-REVIEWED | Posted: 8 December 2021 doi:10.20944/preprints202112.0128.v1

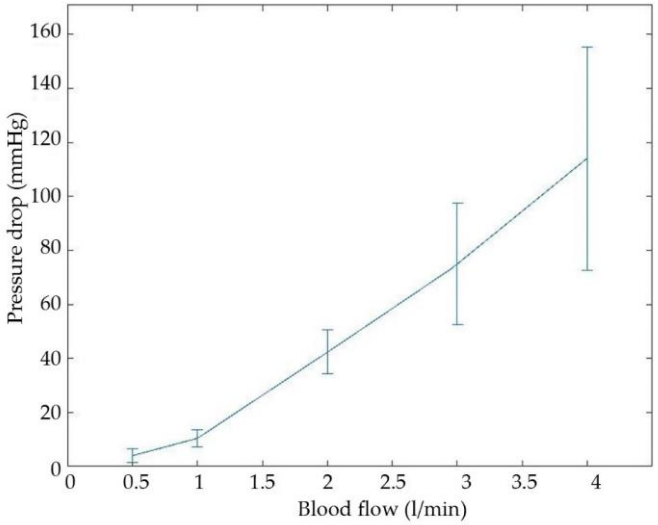

Figure 7 *- In-vitro pressure drop in novel stacked membrane oxygenator using heparinized porcine blood, n = 5, mean and SD*

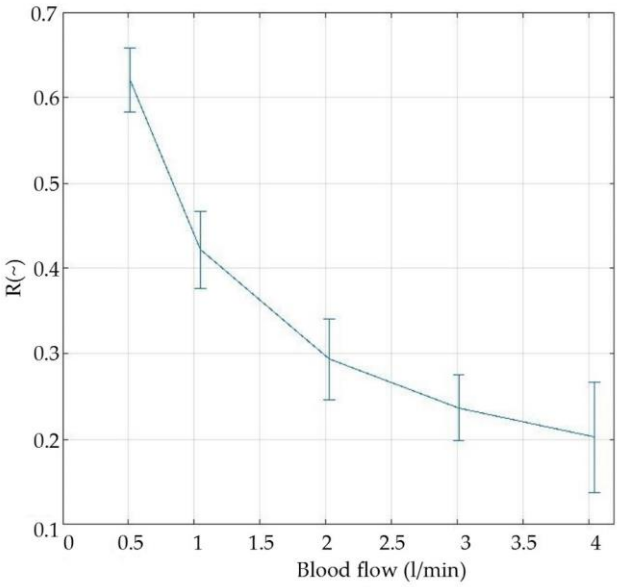

Figure 8 - *Heat transfer efficacy depicted as R-value (according to ISO 7199 [25]), n = 10, mean and SD*

Preprints (www.preprints.org) | NOT PEER-REVIEWED | Posted: 8 December 2021 doi:10.20944/preprints202112.0128.v1

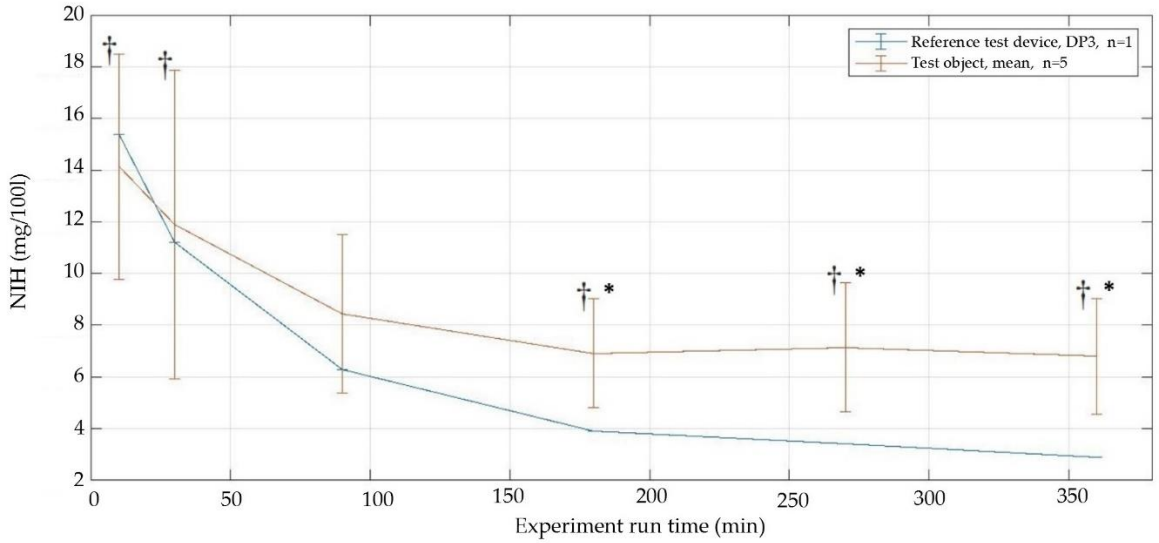

Figure 9 *- In-vitro hemolysis results depicted as normalized index of hemolysis (NIH), mean and SD. The predicate device is depicted in blue (n = 1, iLA oxygenator, DP3 pump), the test devices are depicted in red (n = 5).* ✝*: Normal distribution (tested with Kolmogorov-Smirnov), *: significant difference between test device and predicate (two-tailed one sample t-test, p < 0.05 for Gaussian distributions). The non-Gaussian distribution at t = 90 min was not further analyzed due to small sample size*

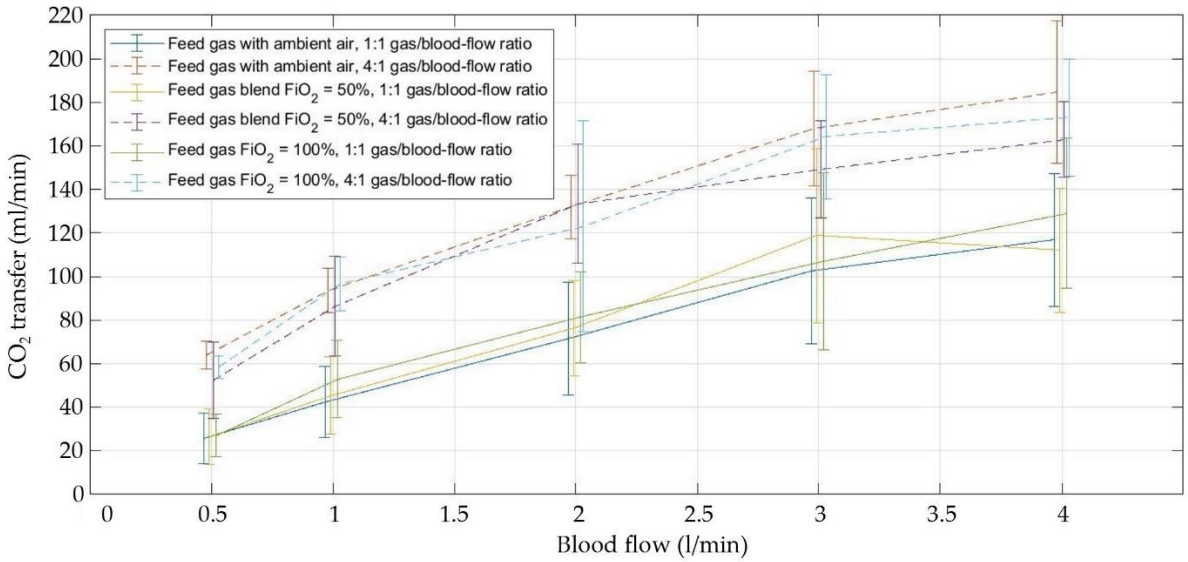

Figure 10 - *Carbon dioxide transfer rates for different feed gas blends and gas/blood-flow ratios, n = 5, mean and SD*

Preprints (www.preprints.org) | NOT PEER-REVIEWED | Posted: 8 December 2021 doi:10.20944/preprints202112.0128.v1

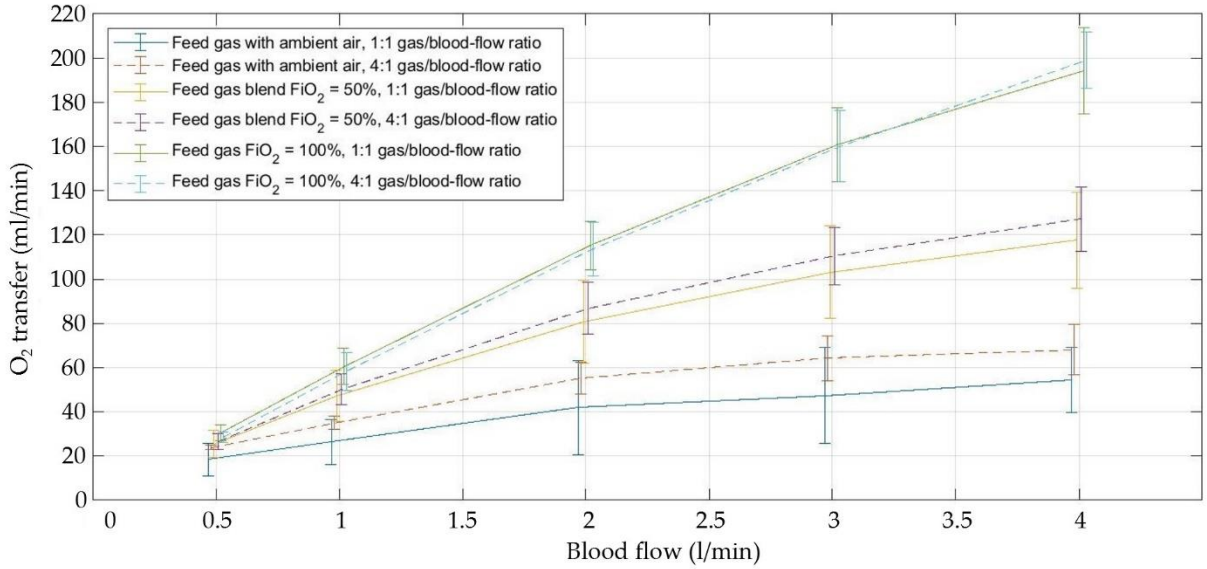

Figure 11 *- Oxygen transfer rates for different feed gas blends and gas/blood-flow ratios, n = 5, mean and SD*

3.2. In-vivo evaluation

A total of six pigs were put on the dedicated ECMO system and treated following the protocol described above. All animals survived until the planned termination of the experiment. Five animals had stable vital parameters during each stage, reaching a respiratory rate as low as 8 min^{-1} and a mean F_iO_2 of 18 %. The sixth animal did not reach a respiratory rate of 8 min^{-1} in the supine position, but in the Trendelenburg position. Throughout all experiments, the heart rate remained stable for three of the five experimental stages and increased during the last sequences of both supine and 45° reverse Trendelenburg position. The mean arterial pressure showed no conclusive trend. The mean pulmonary artery pressure changed only due to the 45° reverse Trendelenburg positioning, by an average decrease of 10 mmHg. Due to anesthesia and the resulting lack of vasoconstriction, sufficient vital parameters could not be sustained below a respiratory rate of 10 min^{-1} during the 45° reverse Trendelenburg position, despite abdominal compression. The ACT was kept above 150 s as targeted. Neither bleeding nor macroscopically or clinically observable thrombosis occurred during the experiments. The hemoglobin was mostly kept between 9 and 11 g/dl. There was no technical failure with any of the components.

Table 1 shows the measured data from intermittent mechanical ventilation, vital parameters, ECMO settings, and blood gas analysis.

Preprints (www.preprints.org) | NOT PEER-REVIEWED | Posted: 8 December 2021 doi:10.20944/preprints202112.0128.v1

Table 1 *- Animal trial monitoring. Supine: animal was positioned flat on the back; Trend: 45° reverse Trendelenburg position, simulating a mobilized patient; 12,10,8: respiratory rate of the intermittent mechanical ventilation, simulating hypercapnic respiratory failure. RMV=respiratory minute volume; F_iO_2 = fraction of inspired oxygen, utilized for simulating hypoxemic respiratory failure; HF = heart frequency; MAP = mean arterial pressure (approximated from end-systolic and end-diastolic pressures); MPAP = mean pulmonary arterial pressure (approximated); S = oxygen saturation, p = partial pressures, et = end tidal/respiratory, ΔP = membrane pressure drop; fPHb = free plasma hemoglobin; V = gas transfer. Indices: a = arterial, v = mixed venous at pulmonary artery, cv = mixed venous at vena cava superior. Carbon dioxide blood contents were calculated using a function by Douglas et al. [29] with a CO_2-plasma diffusion coefficient of 0.03 mmol/mmHg and an apparent dissociation constant of carbonic acid of 6.1. Oxygen contents were calculated using a function by Leach et al. [30] with the Hüfner-number = 1.34 and with an O_2-plasma diffusion coefficient of 0.03 ml/mmHg/dl. Significance was tested for all groups using the Friedman test with Dunn's post test. (0): No significance between any combination of groups using Dunn's; (1): Supine 8 was significantly different to Supine 12 and Trend 12 using Dunn's. If values were missing within a parameter set, Kruskal-Wallis test was conducted. No parameter and combination of tested groups showed significance for p<0.05, except for the controlled parameter F_iO_2. The column p-value shows the Friedman/Kruskal-Wallis results*

		Supine 12			Supine 10			Supine 8			Trend 12			Trend 10			p-value
Parameter	**Unit**	Mean	Median	SD	Mean	Median	SD	Mean	Median	SD	Mean	Median	SD	Mean	Median	SD	* = Friedmann †= Kruskar-Wallis (i) = Dunn's post
RMV	l/min	4	5	2	4	4	1	3	3	2	5	5	1	5	4	1	0.040 *, (0)
F_iO_2	%	21	21	1	20	20	3	18	18	0	21	21	1	20	19	1	0.004 *, (1)
HF	1/min	119	111	34	119	121	51	151	169	56	166	168	40	171	171	36	0.035 *, (0)
MAP	mmHg	75	71	14	105	94	38	94	84	18	79	75	20	71	71	15	0.040 *, (0)
MPAP	mmHg	22	20	8	24	21	10	24	23	5	14	14	12	17	15	16	0.355 *, (0)
S_aO_2	%	84	87	11	80	85	14	73	77	24	83	87	10	73	74	11	0.483 †
$S_{cv}O_2$	%	71	72	10	61	67	13	52	61	17	56	56	7	57	54	11	0.235 †
S_vO_2	%	65	67	6	68	72	13	55	62	18	57	58	5	56	55	4	0.231 †
p_aO_2	mmHg	66	64	15	67	67	19	54	50	19	62	65	10	52	50	8	0.311 †
$p_{cv}O_2$	mmHg	49	47	6	43	43	5	60	40	35	40	42	3	41	40	4	0.157 †
p_vO_2	mmHg	44	44	2	50	45	12	38	39	5	40	41	3	40	40	3	0.075 †
p_aCO_2	mmHg	53	55	5	49	50	8	49	45	13	50	49	7	53	51	8	0.556 †
$p_{cv}CO2$	mmHg	58	58	5	57	58	6	56	48	16	57	56	6	59	55	10	0.873 †
p_vCO_2	mmHg	56	55	5	52	51	7	51	47	16	54	53	7	57	56	9	0.744 †
$etCO_2$	%	7	6	1	6	7	2	7	6	1	7	7	1	7	7	1	0.747 *
Arterial lactate	mmol/l	2.8	1.0	4.1	3.5	1.7	4.1	3.0	1.8	2.7	4.1	2.6	4.0	5.6	4.5	4.8	0.255
Arterial pH	[]	7.4	7.4	0.1	7.4	7.4	0.1	7.4	7.4	0.1	7.4	7.4	0.1	7.3	7.3	0.1	0.321 †
Blood flow ECMO	ml/min	1	2	1	2	2	1	2	2	1	1	2	1	2	2	0	0.045 *, (0)
Pump speed	1/min	5470	5617	2878	6803	7188	2287	7457	7992	1774	5797	6967	2647	8097	8100	1581	0.082 *
Gas flow	l/min	4	4	4	5	4	3	6	6	3	4	4	3	5	5	3	0.749 *
F_iO_2 ECMO	%	68	100	43	86	100	23	100	100	0	74	100	41	100	100	0	0.171 *
ΔP ECMO	mmHg	7	7	13	18	20	14	30	28	16	12	16	15	23	26	10	0.075 *
fPHb	mg/dl	15	13	6	12	12	7	12	12	7	14	12	4	13	14	6	0.920 *
SO_2 post ECMO	%	96	100	8	100	100	1	98	100	5	98	100	3	100	100	0	0.922 *
SO_2 pre ECMO	%	69	76	10	63	68	12	55	58	14	64	68	9	56	55	5	0.323 *
pO_2 post ECMO	mmHg	278	322	199	239	227	86	223	182	125	228	232	139	234	181	107	0.736 *
pO_2 pre ECMO	mmHg	48	50	5	48	45	11	52	40	27	45	46	4	41	40	2	0.171 *
pCO_2 post ECMO	mmHg	38	37	13	36	36	5	40	36	7	37	36	3	41	41	3	0.073 *
pCO_2 pre ECMO	mmHg	58	60	5	54	56	8	54	51	11	55	55	6	59	57	8	0.294 *

Preprints (www.preprints.org) | NOT PEER-REVIEWED | Posted: 8 December 2021 doi:10.20944/preprints202112.0128.v1

VCO_2 ECMO	ml/min	106	69	126	85	86	28	78	88	41	58	57	29	60	55	20	0.255 *
VO_2 ECMO	ml/min	56	57	48	90	93	49	122	133	45	69	74	46	116	123	32	0.220 *

The ECMO blood flow was mostly well below its functional limit, with a maximum flow of 3 l/min for a total of only 2 hours in a single animal. A higher blood flow could not be achieved during the experiments due to a combination of venous insufficiency and suction at the small inlet diameter of double lumen cannula. This resulted in very low arterial oxygen saturation S_aO_2 between 40 % and 95 %. It can also be seen that the venous saturations S_vO_2 are very low as well and decreasing with progression through the experimental sequences. **Figure 12** shows the difference between arterial and venous oxygen saturation in all experimental sequences. The course of the oxygen saturation and the lactate levels suggest a progressing oxygen debt. At the same time, the blood gas analysis at the oxygenator outlet showed saturations well above 90 % while partial oxygen pressures at the inlet mostly were between 40 and 70 mmHg. The oxygen transfer over the membrane oxygenator stays above 56 ml/min on average and increases to an average of 122 ml/min for higher ECMO blood flows. The respective carbon dioxide elimination ranges between 58 and 106 ml/min.

In contrast to the O_2-values that decrease with progression of the experimental sequences, the venous CO_2-levels stay relatively stable between 45 and 75 mmHg. The CO_2-elimination even increases with progression of the experimental sequences in supine position and decreases in 45° reverse Trendelenburg position. **Figure 13** shows the courses of the venous and arterial pCO_2. Simultaneously, the pCO_2-elimination in the ECMO-circuit effectively lowers the pCO_2 from between 50 - 65 mmHg to around 25 - 45 mmHg. Throughout all experiments, the pH-values mostly remained between 7.2 and 7.5.

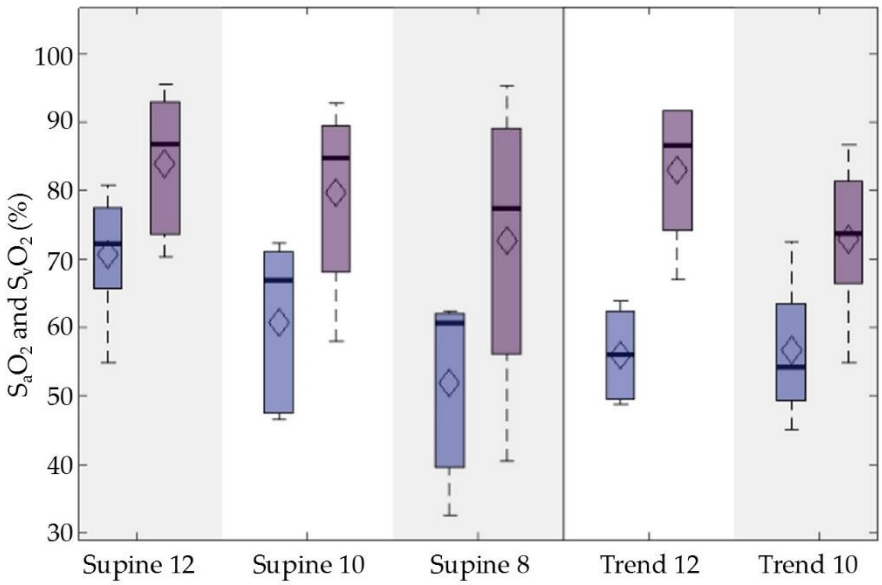

***Figure 12** - **Mixed venous and arterial oxygen saturations** for supine position and reverse Trendelenburg. Each column depicts one group of the experimental sequence. Blue depicts venous values, purple depicts arterial values. Boxplots show 95%-CI (whiskers), 50 % interval (box), median (black bar), mean (diamond)*

Preprints (www.preprints.org) | NOT PEER-REVIEWED | Posted: 8 December 2021 doi:10.20944/preprints202112.0128.v1

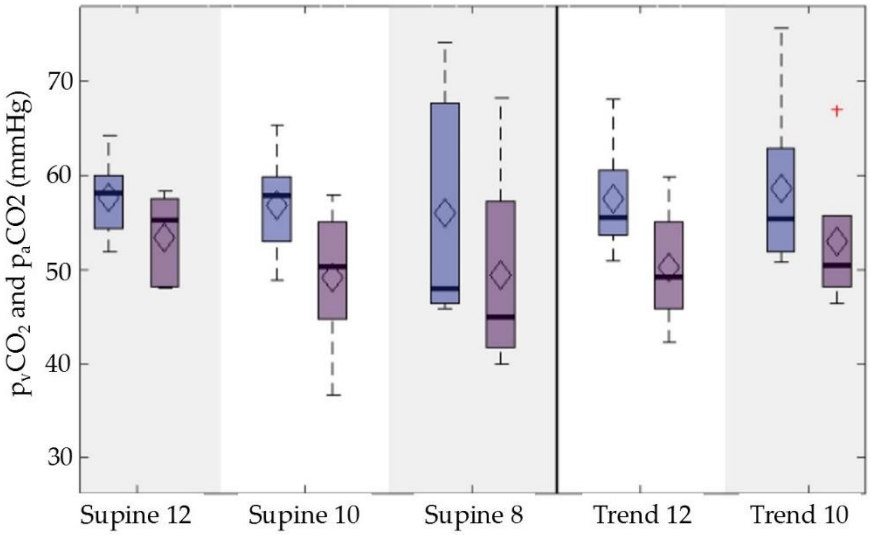

Figure 13 - Mixed venous and arterial carbon dioxide partial pressures *for supine position and reverse Trendelenburg ("Trend"). Each column depicts one group of the experimental sequence. Blue depicts venous values, purple depicts arterial values. Boxplots show 95%-CI (whiskers), 50 %-interval (box), median (black bar), mean (diamond), outlier (red cross)*

The ECMO parameters reflect the cannula related issues to achieve a flow of 3 l/min and the concept to run the ECMO circulation as low as possible. The ECMO blood flow was increased with the reduction of ventilator settings from on average 1.3 l/min to 2.3 l/min and ranged between 500 ml/min and 3 l/min. **Figure 14** shows the corresponding box plots. Moreover, it was intended to run the ECMO with initial oxygen fractions of ambient air and increase with physiologic demand. It can be seen that the oxygen fraction was increased early to 100 % with decreasing ventilator settings. **Figure 15** shows the ECMO oxygen fraction over the course of the experiments as boxplots.

Preprints (www.preprints.org) | NOT PEER-REVIEWED | Posted: 8 December 2021 doi:10.20944/preprints202112.0128.v1

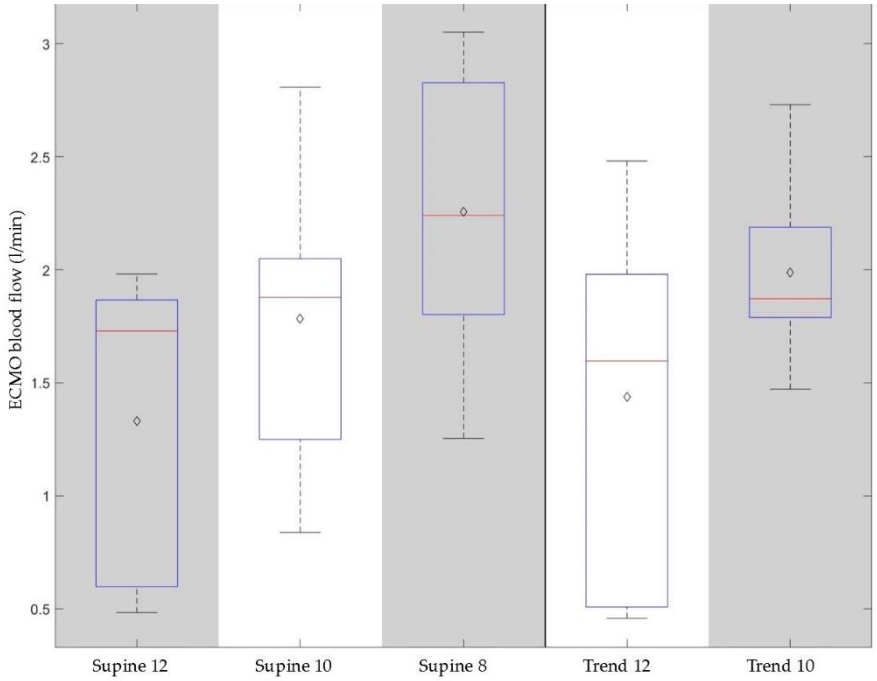

Figure 14 - ECMO blood flow *for supine position (left) and reverse Trendelenburg (right). Each column depicts one group of the experimental sequence. Boxplots show 95%-CI (whiskers), 50 %-interval (box), median (red bar), mean (diamond)*

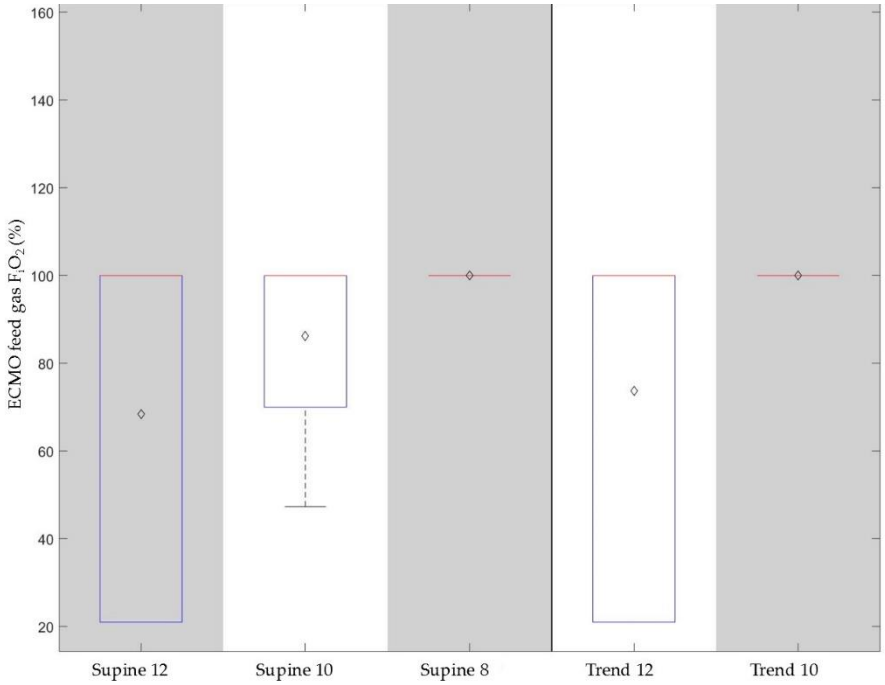

Figure 15 - ECMO feed gas oxygen fraction *for supine position (left) and reverse Trendelenburg (right). Each column depicts one group of the experimental sequence. Boxplots show 95%-CI (whiskers), 50 %-interval (box), median (red bar), mean (diamond)*

Finally, the pressure drop in all six oxygenators proved to be around 60 % of the values determined in vitro; that means that the pressure drop at 3 l/min was between 40 and 50 mmHg drop (compared to 50 to 100 mmHg in vitro). Hemolysis was measured as

Preprints (www.preprints.org) | NOT PEER-REVIEWED | Posted: 8 December 2021 doi:10.20944/preprints202112.0128.v1

change of free plasma hemoglobin and showed no increase in any animal. Values stayed in a range of 4 - 22 mg/dl.

4. Discussion

A novel veno-venous ECMO system with downsized and integrated components dedicated for patient mobilization was tested in vitro and in vivo.

4.1. In-vitro evaluation

The system was tested for hemolysis, membrane pressure drop, as well as heat and gas transfer for the intended use case. Heat and gas transfer achieved targeted values. Target oxygen transfer rates were realized only at pure oxygen for both 1 : 1 and 4 : 1 flow ratio gas/blood. Target CO_2-transfer rates were reached only with 4 : 1 flow ratio, independent of oxygen fraction. These results were anticipated, though lower required oxygen fractions would strengthen the use case of the device. Ficial et al. [31] recently hypothesized that a higher F_iO_2 in the ECMO circuit may translate into higher CO_2 transfer rates by displacing CO_2 from HCO_3^-; our data do not support this theory, at least not in clinically relevant dimensions.

The pressure drop was relatively high in vitro but comparable to commercial devices in vivo. Hemolysis was three times as high as in the predicate device. The prototype status of the oxygenator may have caused a significant increase in hemolysis, because the entire casing was printed. Recently, Petersdorff-Campen et al. [32] showed an increase in hemolysis in printed blood pumps of 620 %, which may explain our results. Last, we have successfully used a mobile gas blender that allows quick, individual, and automatable gas mixtures of medical oxygen and ambient air.

4.2. In-vivo evaluation

The in-vivo model was designed with three characteristic features. First, the hypoxic and hypercapnic respiratory failure was simulated using the respiratory rate and oxygen fraction of the intermittent mechanical ventilator. Both hypoxia and the hypercapnia could effectively be established in a controllable and stable manner. Second, the animal was switched from supine position to 45° reverse Trendelenburg position, with the aim to simulate an upright awake patient. Established animal models for ECMO testing are using recumbent position [33] or sometimes quadruped position [34,35], which do not reflect the hemodynamic changes of an upright patient. The anesthesia prohibited effective physiologic autoregulation, especially vasoconstriction, so that we actually simulated a distributive hypovolemic shock. We had to counteract this shock by compressing the abdomen of the pig. This model is not yet established through these experiments, but we showed feasibility. Additionally, as can be seen by the deteriorated sitting pig, the model may be of high relevance for the simulated mobilized ECMO patient. And third, we tried to blend ambient air with medical oxygen. Our data suggests that situations with a low oxygen demand may allow for resource saving gas blending, e.g. for more CO_2-removal focused applications. Ideally, in combination with an automated control, the device measures oxygen and carbon dioxide levels in high frequency and adapts oxygen fraction and total gas flow continuously; an according system has been published by our colleagues before [28]. With respect to our in-vitro data, we could confirm that a high gas flow eliminates CO_2 effectively. For $ECCO_2R$-patients mainly suffering from hypercapnic respiratory failure, the mobile gas blender may offer large range extension.

In the experiments, severely hypoxic and hypercapnic animals were observed. The most limiting factor was the drainage insufficiency due to the small cannula size that prohibited higher ECMO flows. The optimal flow regime of the cannula is 1 to 1.5 l/min, i.e. half of the intended operating point. This caused low inlet pressures. Further, the NovaPort Twin cannula has only a single drainage opening either in superior or inferior vena cava. Both factors contribute to a limit in ECMO flow. Alternative cannulas, e. g. the Avalon cannula, are used for walking ECMO in a clinical setting and enable higher blood flow and consecutive oxygen transfer, but application is limited due to high dislocation

risk [36–38]. We therefore conclude that the cannula was not well chosen for the intended use. In consequence, we were not able to show the functional limit of the membrane oxygenator unit. The safe utilization of existing cannulae in different inlet- and outlet positions in the relevant vessels remains to be investigated, especially with respect to the altered hemodynamics of a sitting or mobilized patient. However, new concepts for patient-ECMO interfaces seem necessary to provide efficient gas transfer rates and simultaneously safe mobilization of the patient [39].

Blood gas analyses directly before and after the fiber bundle proved an effective gas transfer. Other contributive factors for the severe hypoxia and hypercapnia were, firstly, the low hemoglobin levels of around 10 g/dl. Secondly, the extracorporeal circulation may have been partly recirculating freshly oxygenated and decarboxylated blood; this phenomenon is common [40] and decreases the effective blood flow almost by the fraction of the recirculating blood [41,42]. This theory is supported strongly, as all venous samples (pre-oxygenator, vena cava superior and pulmonary artery) are almost identical. If no relevant recirculation occurred, the pre-oxygenator pCO_2 would have to be much lower (and pO_2 higher), based on the high post-oxygenator gas values. Instead, relatively homogenously distributed blood fractions are reentering the extracorporeal circuit and passing through the right heart. For the current proof of concept study, we aimed at a low ECMO support. In theory, a lower support means less utilization of resources. The current study reflects the borderline of low flow within the applied animal model. While this was a plausible approach for the present study, it is necessary to run the system at an operating point prohibiting harmfully high carbon dioxide levels and a profound oxygen debt.

The gas transfer rates ECMO VCO_2 and ECMO VO_2 showed very similar results to the in-vitro tests for the respective blood flows. Müller et al. [43] as well as Kopp et al. [44] stated that 150 ml/min CO_2-elimination is required to reach around 50 % of the production for an $ECCO_2R$ scenario. We showed in our in-vitro test higher values of around 160 ml/min; our in-vivo test confirmed the results within the limited blood flow range due to the cannula.

4.3. Conclusion

Overall, we could show that the downsizing of an ECMO system with a carrying system close to the body, autonomous gas and energy supply as well as a control system is feasible. With the chosen cannula, the system was running rather like an $ECCO_2R$ device. A correctly selected cannula is obligatory to provide higher blood flow and, consecutively, higher oxygen transfer. Using a novel large animal model, we further showed the feasibility of a system applicable to mobilize patients and inherently established an appropriate in-vivo model. We suggest progressing with the technology and the concept of mobilization.

~~**Supplementary Materials:** The following are available online at www.mdpi.com/xxx/s1, Figure S1: title, Table S1: title, Video S1: title.~~

Author Contributions: For research articles with several authors, a short paragraph specifying their individual contributions must be provided. The following statements should be used "Conceptualization, R.K., U.S., T.S., P.S., G.W., S.J., and J.A.; methodology, R.K., H.L., U.S., T.S., P.S., G.W., N.S. and J.A.; software, B.S.; validation, J.P., P.S., L.Sc., B.S., G.W. and N.S.; formal analysis, B.S., R.K., S.J. and L.J.S. ; investigation, P.S., B.S., N.S., J.P., H.L., L.Sc, and G.W.; resources, T.S., R.K., J.A., and U.S.; data curation, B.S., L.J.S., and S.J.; writing—original draft preparation, L.J.S., R.K.; writing—review and editing, R.K., U.S., J.A., N.S., T.S. and S.J; visualization, L.J.S., B.S.; supervision, U.S., J.A., and R.K.; project administration, P.W., and G.W.; funding acquisition, U.S., T.S., J.A., and R.K. All authors have read and agreed to the published version of the manuscript." Please turn to the CRediT taxonomy for the term explanation. Authorship must be limited to those who have contributed substantially to the work reported.

Funding: This research was funded by the Federal Ministry of Education and Research (BMBF), grant number 13GW0046B.

Institutional Review Board Statement: Permission for the experiments was granted by the governmental animal care committee (Landesamt für Natur, Umwelt und Verbraucherschutz

Nordrhein-Westfalen, Recklinghausen, Germany, ref. no. 84-02.04.2016.A472), and the implementation followed the principles of laboratory animal care.

References

1. Tramm, R.; Ilic, D.; Davies, A.R.; Pellegrino, V.A.; Romero, L.; Hodgson, C. Extracorporeal membrane oxygenation for critically ill adults. *Cochrane Database Syst. Rev.* **2015**, *1*, CD010381, doi:10.1002/14651858.CD010381.pub2.
2. Weill, D.; Benden, C.; Corris, P.A.; Dark, J.H.; Davis, R.D.; Keshavjee, S.; Lederer, D.J.; Mulligan, M.J.; Patterson, G.A.; Singer, L.G.; et al. A consensus document for the selection of lung transplant candidates: 2014--an update from the Pulmonary Transplantation Council of the International Society for Heart and Lung Transplantation. *J. Heart Lung Transplant.* **2015**, *34*, 1–15, doi:10.1016/j.healun.2014.06.014.
3. Benazzo, A.; Schwarz, S.; Frommlet, F.; Schweiger, T.; Jaksch, P.; Schellongowski, P.; Staudinger, T.; Klepetko, W.; Lang, G.; Hoetzenecker, K. Twenty-year experience with extracorporeal life support as bridge to lung transplantation. *J. Thorac. Cardiovasc. Surg.* **2019**, *157*, 2515-2525.e10, doi:10.1016/j.jtcvs.2019.02.048.
4. Biscotti, M.; Gannon, W.D.; Agerstrand, C.; Abrams, D.; Sonett, J.; Brodie, D.; Bacchetta, M. Awake Extracorporeal Membrane Oxygenation as Bridge to Lung Transplantation: A 9-Year Experience. *Ann. Thorac. Surg.* **2017**, *104*, 412–419, doi:10.1016/j.athoracsur.2016.11.056.
5. Fuehner, T.; Kuehn, C.; Hadem, J.; Wiesner, O.; Gottlieb, J.; Tudorache, I.; Olsson, K.M.; Greer, M.; Sommer, W.; Welte, T.; et al. Extracorporeal membrane oxygenation in awake patients as bridge to lung transplantation. *Am. J. Respir. Crit. Care Med.* **2012**, *185*, 763–768, doi:10.1164/rccm.201109-1599OC.
6. Hoetzenecker, K.; Donahoe, L.; Yeung, J.C.; Azad, S.; Fan, E.; Ferguson, N.D.; Del Sorbo, L.; Perrot, M. de; Pierre, A.; Yasufuku, K.; et al. Extracorporeal life support as a bridge to lung transplantation-experience of a high-volume transplant center. *J. Thorac. Cardiovasc. Surg.* **2018**, *155*, 1316-1328.e1, doi:10.1016/j.jtcvs.2017.09.161.
7. Quaderi, S.A.; Hurst, J.R. The unmet global burden of COPD. *Glob. Health Epidemiol. Genom.* **2018**, *3*, e4, doi:10.1017/gheg.2018.1.
8. Varmaghani, M.; Dehghani, M.; Heidari, E.; Sharifi, F.; Moghaddam, S.S.; Farzadfar, F. Global prevalence of chronic obstructive pulmonary disease: systematic review and meta-analysis. *East. Mediterr. Health J.* **2019**, *25*, 47–57, doi:10.26719/emhj.18.014.
9. Chambers, D.C.; Cherikh, W.S.; Harhay, M.O.; Hayes, D.; Hsich, E.; Khush, K.K.; Meiser, B.; Potena, L.; Rossano, J.W.; Toll, A.E.; et al. The International Thoracic Organ Transplant Registry of the International Society for Heart and Lung Transplantation: Thirty-sixth adult lung and heart-lung transplantation Report-2019; Focus theme: Donor and recipient size match. *J. Heart Lung Transplant.* **2019**, *38*, 1042–1055, doi:10.1016/j.healun.2019.08.001.
10. Shah, R.J.; Kotloff, R.M. Lung transplantation for obstructive lung diseases. *Semin. Respir. Crit. Care Med.* **2013**, *34*, 288–296, doi:10.1055/s-0033-1348468.
11. Kozower, B.D.; Meyers, B.F.; Smith, M.A.; Oliveira, N.C. de; Cassivi, S.D.; Guthrie, T.J.; Wang, H.; Ryan, B.J.; Shen, K.R.; Daniel, T.M.; et al. The impact of the lung allocation score on short-term transplantation outcomes: a multicenter study. *J. Thorac. Cardiovasc. Surg.* **2008**, *135*, 166–171, doi:10.1016/j.jtcvs.2007.08.044.
12. Turner, D.A.; Cheifetz, I.M.; Rehder, K.J.; Williford, W.L.; Bonadonna, D.; Banuelos, S.J.; Peterson-Carmichael, S.; Lin, S.S.; Davis, R.D.; Zaas, D. Active rehabilitation and physical therapy during extracorporeal membrane oxygenation while awaiting lung transplantation: a practical approach. *Crit. Care Med.* **2011**, *39*, 2593–2598, doi:10.1097/CCM.0b013e3182282bbe.
13. Cypel, M.; Keshavjee, S. Extracorporeal life support as a bridge to lung transplantation. *Clin. Chest Med.* **2011**, *32*, 245–251, doi:10.1016/j.ccm.2011.02.005.

14. Jonghe, B. de; Sharshar, T.; Lefaucheur, J.-P.; Authier, F.-J.; Durand-Zaleski, I.; Boussarsar, M.; Cerf, C.; Renaud, E.; Mesrati, F.; Carlet, J.; et al. Paresis acquired in the intensive care unit: a prospective multicenter study. *JAMA* **2002**, *288*, 2859–2867, doi:10.1001/jama.288.22.2859.
15. Needham, D.M.; Korupolu, R.; Zanni, J.M.; Pradhan, P.; Colantuoni, E.; Palmer, J.B.; Brower, R.G.; Fan, E. Early physical medicine and rehabilitation for patients with acute respiratory failure: a quality improvement project. *Arch. Phys. Med. Rehabil.* **2010**, *91*, 536–542, doi:10.1016/j.apmr.2010.01.002.
16. Truong, A.D.; Fan, E.; Brower, R.G.; Needham, D.M. Bench-to-bedside review: mobilizing patients in the intensive care unit--from pathophysiology to clinical trials. *Crit. Care* **2009**, *13*, 216, doi:10.1186/cc7885.
17. Crotti, S.; Iotti, G.A.; Lissoni, A.; Belliato, M.; Zanierato, M.; Chierichetti, M.; Di Meo, G.; Meloni, F.; Pappalettera, M.; Nosotti, M.; et al. Organ allocation waiting time during extracorporeal bridge to lung transplant affects outcomes. *Chest* **2013**, *144*, 1018–1025, doi:10.1378/chest.12-1141.
18. Lehr, C.J.; Zaas, D.W.; Cheifetz, I.M.; Turner, D.A. Ambulatory extracorporeal membrane oxygenation as a bridge to lung transplantation: walking while waiting. *Chest* **2015**, *147*, 1213–1218, doi:10.1378/chest.14-2188.
19. Abrams, D.; Combes, A.; Brodie, D. Extracorporeal membrane oxygenation in cardiopulmonary disease in adults. *J. Am. Coll. Cardiol.* **2014**, *63*, 2769–2778, doi:10.1016/j.jacc.2014.03.046.
20. Abrams, D.; Javidfar, J.; Farrand, E.; Mongero, L.B.; Agerstrand, C.L.; Ryan, P.; Zemmel, D.; Galuskin, K.; Morrone, T.M.; Boerem, P.; et al. Early mobilization of patients receiving extracorporeal membrane oxygenation: a retrospective cohort study. *Crit. Care* **2014**, *18*, R38, doi:10.1186/cc13746.
21. Abrams, D.; Madahar, P.; Eckhardt, C.M.; Short, B.; Yip, N.H.; Parekh, M.; Serra, A.; Dubois, R.L.; Saleem, D.; Agerstrand, C.; et al. Early Mobilization during ECMO for Cardiopulmonary Failure in Adults: Factors Associated with Intensity of Treatment. *Ann. Am. Thorac. Soc.* **2021**, doi:10.1513/AnnalsATS.202102-151OC.
22. Ko, Y.; Cho, Y.H.; Park, Y.H.; Lee, H.; Suh, G.Y.; Yang, J.H.; Park, C.-M.; Jeon, K.; Chung, C.R. Feasibility and Safety of Early Physical Therapy and Active Mobilization for Patients on Extracorporeal Membrane Oxygenation. *ASAIO J.* **2015**, *61*, 564–568, doi:10.1097/MAT.0000000000000239.
23. Pruijsten, R.; van Thiel, R.; Hool, S.; Saeijs, M.; Verbiest, M.; Reis Miranda, D. Mobilization of patients on venovenous extracorporeal membrane oxygenation support using an ECMO helmet. *Intensive Care Med.* **2014**, *40*, 1595–1597, doi:10.1007/s00134-014-3410-9.
24. Haji, J.Y.; Mehra, S.; Doraiswamy, P. Awake ECMO and mobilizing patients on ECMO. *Indian J. Thorac. Cardiovasc. Surg.* **2021**, 1–10, doi:10.1007/s12055-020-01075-z.
25. ISO. *Cardiovascular implants and artificial organs*: *Cardiovascular implants and artificial organs — Blood-gas exchangers (oxygenators)*, *11.040.40 Implants for surgery, prosthetics and orthotics* (7199:2016).
26. Food and Drug Administration. *Guidance for Cardiopulmonary Bypass Oxygenators 510 (k) Submissions*: *Final Guidance for Industry and FDA Staff*, 2010.
27. Hesselmann, F.; Focke, J.M.; Schlanstein, P.C.; Steuer, N.B.; Kaesler, A.; Reinartz, S.D.; Schmitz-Rode, T.; Steinseifer, U.; Jansen, S.V.; Arens, J. Introducing 3D-potting: a novel production process for artificial membrane lungs with superior blood flow design. *Bio-des. Manuf.* **2021**, doi:10.1007/s42242-021-00139-2.
28. Kopp, R.; Bensberg, R.; Stollenwerk, A.; Arens, J.; Grottke, O.; Walter, M.; Rossaint, R. Automatic Control of Veno-Venous Extracorporeal Lung Assist. *Artif. Organs* **2016**, *40*, 992–998, doi:10.1111/aor.12664.
29. Douglas, A.R.; Jones, N.L.; Reed, J.W. Calculation of whole blood CO2 content. *J. Appl. Physiol. (1985)* **1988**, *65*, 473–477, doi:10.1152/jappl.1988.65.1.473.
30. Leach, R.M.; Treacher, D.F. The pulmonary physician in critical care * 2: oxygen delivery and consumption in the critically ill. *Thorax* **2002**, *57*, 170–177, doi:10.1136/thorax.57.2.170.

31. Ficial, B.; Vasques, F.; Zhang, J.; Whebell, S.; Slattery, M.; Lamas, T.; Daly, K.; Agnew, N.; Camporota, L. Physiological Basis of Extracorporeal Membrane Oxygenation and Extracorporeal Carbon Dioxide Removal in Respiratory Failure. *Membranes (Basel)* **2021**, *11*, doi:10.3390/membranes11030225.
32. Petersdorff-Campen, K. von; Abeken, J.; Zélicourt, D. de; Kurtcuoglu, V.; Meboldt, M.; Schmid Daners, M. In Vitro Testing and Comparison of Additively Manufactured Polymer Impellers for the CentriMag Blood Pump. *ASAIO J.* **2021**, *67*, 306–313, doi:10.1097/MAT.0000000000001220.
33. Kopp, R.; Bensberg, R.; Arens, J.; Steinseifer, U.; Schmitz-Rode, T.; Rossaint, R.; Henzler, D. A miniaturized extracorporeal membrane oxygenator with integrated rotary blood pump: preclinical in vivo testing. *ASAIO J.* **2011**, *57*, 158–163, doi:10.1097/MAT.0b013e31820bffa9.
34. Madhani, S.P.; Frankowski, B.J.; Ye, S.-H.; Burgreen, G.W.; Wagner, W.R.; Kormos, R.; D'Cunha, J.; Federspiel, W.J. In Vivo 5 Day Animal Studies of a Compact, Wearable Pumping Artificial Lung. *ASAIO J.* **2019**, *65*, 94–100, doi:10.1097/MAT.0000000000000740.
35. Kopp, R.; Mottaghy, K.; Kirschfink, M. Mechanism of complement activation during extracorporeal blood-biomaterial interaction: effects of heparin coated and uncoated surfaces. *ASAIO J.* **2002**, *48*, 598–605, doi:10.1097/00002480-200211000-00005.
36. Kalbhenn, J.; Maier, S.; Heinrich, S.; Schallner, N. Bedside repositioning of a dislocated Avalon-cannula in a running veno-venous ECMO. *J. Artif. Organs* **2017**, *20*, 285–288, doi:10.1007/s10047-017-0961-x.
37. Chen, R.H.-S.; Yam, N.; Lun, K.-S.; Au, T.W.-K. Migrated Avalon-Elite cannula in an infant transcatheter repositioning without interruption of ECMO flow. *J. Artif. Organs* **2021**, *24*, 382–386, doi:10.1007/s10047-020-01238-0.
38. Single or Double Site Cannuation for Veno-Venous Ecmo in Severe Obese Patient? *ARC Journal of Anesthesiology* **2016**, *1*, doi:10.20431/2455-9792.0104004.
39. Steuer, N.B.; Hugenroth, K.; Beck, T.; Spillner, J.; Kopp, R.; Reinartz, S.; Schmitz-Rode, T.; Steinseifer, U.; Wagner, G.; Arens, J. Long-Term Venovenous Connection for Extracorporeal Carbon Dioxide Removal (ECCO2R)-Numerical Investigation of the Connection to the Common Iliac Veins. *Cardiovasc. Eng. Technol.* **2020**, *11*, 362–380, doi:10.1007/s13239-020-00466-y.
40. Palmér, O.; Palmér, K.; Hultman, J.; Broman, M. Cannula Design and Recirculation During Venovenous Extracorporeal Membrane Oxygenation. *ASAIO J.* **2016**, *62*, 737–742, doi:10.1097/MAT.0000000000000440.
41. Conrad, S.A.; Wang, D. Evaluation of Recirculation During Venovenous Extracorporeal Membrane Oxygenation Using Computational Fluid Dynamics Incorporating Fluid-Structure Interaction. *ASAIO J.* **2021**, *67*, 943–953, doi:10.1097/MAT.0000000000001314.
42. Broman, M.; Frenckner, B.; Bjällmark, A.; Broomé, M. Recirculation during veno-venous extra-corporeal membrane oxygenation--a simulation study. *Int. J. Artif. Organs* **2015**, *38*, 23–30, doi:10.5301/ijao.5000373.
43. Müller, T.; Lubnow, M.; Philipp, A.; Bein, T.; Jeron, A.; Luchner, A.; Rupprecht, L.; Reng, M.; Langgartner, J.; Wrede, C.E.; et al. Extracorporeal pumpless interventional lung assist in clinical practice: determinants of efficacy. *Eur. Respir. J.* **2009**, *33*, 551–558, doi:10.1183/09031936.00123608.
44. Kopp, R.; Bensberg, R.; Wardeh, M.; Rossaint, R.; Kuhlen, R.; Henzler, D. Pumpless arterio-venous extracorporeal lung assist compared with veno-venous extracorporeal membrane oxygenation during experimental lung injury. *Br. J. Anaesth.* **2012**, *108*, 745–753, doi:10.1093/bja/aes021.